Verifying Theories of the Zeeman Effect with the Cadmium Red Line and the Mercury Green Line

Gonghan Xu, Joseph Colosimo

An experiment was carried out to observe the normal and the anomalous Zeeman effects, respectively, for the cadmium red line (643.85nm) and the mercury green line (546.08nm). The polarization of radiations emitted by cadmium under the Zeeman effect agrees with theoretical predictions. Quantification of the spectral lines splittings also agrees with theoretical predictions in a satisfactory manner.

1 Introduction

Along with Röntgen's discovery of X-rays (1895), Bequerel's discovery of radioactivity (1896), and J. J. Thomson's discovery of electron (1897), Pieter Zeeman's discovery of atomic spectral line splittings in the presence of an external magnetic field (1896) unfolded a new era of quantum physics.[1,2] Back in the late 19th century, the idea that electrons are part of an atom was still unclear. The observations of Zeeman's eponymous effect provided crucial evidence that there are particles negatively charged inside atoms and that these particles have the same charge-to-mass ratio as Thomson's cathode ray "corpuscles".[2,3] Besides, the Zeeman effect serves as a useful means for studying the atomic structure, and the anomalous Zeeman effect supplied important clues for Goudsmit and Uhlenbeck to propose the intrinsic spin of electrons.[2,4] Zeeman received the 1902 Nobel Prize in Physics with his mentor Lorentz for their "researches into the influence of magnetism upon radiation phenomena".[5]

As undergraduate students, we performed an experiment to observe the normal and anomalous Zeeman effect, respectively, in splittings of the cadmium red line (643.85nm) and the mercury green line (546.08nm) under an external magnetic field. The goal of this experiment is to verify that the splittings of the spectral lines and their corresponding polarizations agree with theoretical predictions.

2 Theory

This section describes theories that are essential to this experiment.

2.1 LS coupling

Unlike hydrogen, atoms with multiple electrons can have very complicated atomic states due to the mutual electrostatic interactions between the electrons. However, for atoms with a relatively small atomic number (applicable up to around mercury), the atomic state can be well approximated with the LS coupling scheme. The LS coupling scheme focuses on the valence electrons of the atom, where L is the valence electrons' total orbital angular momentum quantum number and S is their total spin quantum number. Given a certain **electronic configuration** of the valence electrons in an atom (this means that each valence electron has well-defined n and l quantum numbers) and assuming that only the valence electrons of the atom can be excited, then LS coupling says that the eigenspaces of the different energy levels of the atom can be approximated by the simultaneous eigenspaces of the valence electrons' total orbital angular momentum operator ($\hat{\vec{L}}^2$) and total spin operator ($\hat{\vec{S}}^2$). So for two atoms of the same type and the same electronic configuration, if the valence electrons of the two atoms have the same quantum numbers L and S, then both atoms should stay in (approximately) the same, well-defined atomic energy levels. On the other hand, if the valence electrons have different L and S quantum number between the two atoms, then the binding energies

of the two atoms will be different. Therefore, with a given electronic configuration, it is helpful to describe an atom with definite L and S quantum numbers for the valence electrons in a **term** of

$$^{2S+1}L \tag{1}$$

where we will write L in spectroscopic notation such that we write "S" for L=0, "P" for L=1, "D" for L=2, "F" for L=3, and so on in alphabetical order. Remember to distinguish the "S" for L=1 from the total spin quantum number S. For example, for an atomic state with S=0 and L=0, the corresponding term is ^1S; for an atomic state with S=1 and L=1, the corresponding term is ^3P.

However, due to spin-orbit interactions within the individual valence electrons, there will be further energy splittings within a term. In this case, we will need to introduce the total angular momentum quantum number J, corresponding to the total angular momentum operator $\hat{\vec{J}}^2 = \left(\hat{\vec{L}}^2 + \hat{\vec{S}}^2\right)^2$, to distinguish the relatively small energy splittings within a term. According to the theory of angular momentum addition in quantum mechanics, we have

$$|L - S| \leq J \leq |L + S| \tag{2}$$

where J can only take values with increments of 1. Therefore, different values of J will split a term further into different **levels** of

$$^{2S+1}L_J \tag{3}$$

where different levels correspond to different energies due to the spin-orbit interactions. In a given level $^{2S+1}L_J$, when there are no more than two valence electrons, there can be 2J+1 **states** with different quantum number M_J, which represents the z-component of the valence electrons' total angular momentum. Without an external magnetic field, different M_J states in the same level will possess the same energy.[6] Only with an external magnetic field (along the z direction) will the different M_J states be resolved.[7] From now on, I will confine our discussion to no more than two valence electrons.

2.2 The Zeeman effect

As described in Section 2.1, when there is no external magnetic field, the atomic energy levels of a relatively light atom can be characterized by its levels $^{2S+1}L_J$. However, if a relatively weak (actually the highest achievable magnetic fields under usual lab conditions are considered relatively week), uniform magnetic field pointing at the +z direction is applied over the atom, then the atom's magnetic dipole moment will interact with this external magnetic field and cause further energy splittings within a level, characterized by the quantum number M_J This is called the Zeeman effect. Here we consider a relatively weak external magnetic field so that the energy contributions from the Zeeman effect (I will call them **Zeeman energies**) are much smaller than those due to the spin-orbit interactions, and thus we can treat the Zeeman effect as a perturbation to a level. Using the perturbation theory, we can obtain the first-order energy correction (the Zeeman energy) for a state $^{2S+1}L_{J,M_J}$ as

$$E_z = g\mu_B B M_J \tag{4}$$

where g is the Landé g factor, μ_B is the Bohr magneton, and B is the magnitude of the external magnetic field. The Landé g factor for a level $^{2S+1}L_J$ is

$$g = \frac{3}{2} + \frac{S(S+1) - L(L+1)}{2J(J+1)} \tag{5}$$

I need to emphasize that the Zeeman effect perturbs the different M_J states in a level $^{2S+1}L_J$ separately. This means that different M_J states in the level have different Zeeman energies E_z, characterized by the quantum number M_J. Therefore, the energy for a level is further split by the external magnetic field, and we say the quantum number M_J is resolved by the external magnetic field. I will call this **Zeeman splitting**.

The direct experimental observation for the Zeeman effect is that the spectral line for an atom that originally corresponds to a transition between two terms will appear to split. Originally, the transition energy for an electron transitioning between two M_J states does not depend on the initial and final values of M_J. However, as the M_J states are resolved by the external magnetic field, the transition energy will now depend on the initial and final values of M_J. Therefore, the original spectral line will split due to the external magnetic field.[7]

2.2.1 Selection rules

To further understand the spectral lines observed under the Zeeman effect, we need to understand the selection rules for LS coupling. The selection rules govern how electrons transition between atomic states. Transitions that obey the selection rules are called **allowed transitions**, while those violating the selection rules are called **forbidden transitions**. The forbidden transitions would still occur, but at a rate much smaller than the allowed transitions.

For the LS coupling scheme, one of the selection rules requires that $\Delta M_J = 0, \pm 1$ (for $\Delta J = 0$, the initial and final M_J cannot be both zero), where $\Delta M_J = M_{J_{\text{final}}} - M_{J_{\text{initial}}}$ Transitions of $\Delta M_J = \pm 1$ are called $\boldsymbol{\sigma}$ **transitions**, while those of $\Delta M_J = 0$ are called $\boldsymbol{\pi}$ **transitions**. The exothermic transitions with $\Delta M_J = 1$ (σ^+ transition) will emit radiations (photons) that are right-circularly polarized with respect to the direction of the external magnetic field. This means that we will see right-circularly polarized light emitted from the atom if the arrow from the atom to us points in the direction of the magnetic field. In contrast, exothermic transitions with $\Delta M_J = -1$ (σ^- transition) and $\Delta M_J = 0$ (π transition) will emit left-circularly polarized light and linearly polarized light polarized along the direction of the magnetic field, respectively. From now on, I will always refer to the direction of the external magnetic field as the +z direction, and I will treat the atom under consideration as staying at the origin of our coordinate system.

Another selection rule for LS coupling that is also relevant to our discussion is $\Delta S = 0$, which means that the total spin quantum number should remain the same between the initial and final states.[8]

2.2.2 The normal Zeeman effect

The normal Zeeman effect refers to when a spectral line splits into three separate lines under the external magnetic field.[9] This happens when the total spin quantum number S for the initial and final states are both zero. In this case, a term will have the same L and J quantum numbers (see Inequality 2), and the Landé g factor for a term, according to Equation 5, becomes 1. According to the selection rules, only transitions of $\Delta M_J = 0, \pm 1$ are allowed. Suppose the atom transitions from State 1 to State 2. Then, according to Equation 4, the Zeeman energy can only contribute an extra transition energy (relative to before the magnetic field was applied) of

$$\begin{aligned} \Delta E_z &= g_2 \mu_B B M_{J_2} - g_1 \mu_B B M_{J_1} \\ &= (g_2 M_{J_2} - g_1 M_{J_1}) \mu_B B \end{aligned} \tag{6}$$

Since both the initial and final states have the Landé g factor of 1, we have

$$\Delta E_z = \Delta M_J \mu_B B \tag{7}$$

where $\Delta M_J = M_{J_2} - M_{J_1}$. By selection rules, ΔM_J can only be 0, ± 1. Therefore, $\Delta E_z = 0$ or $\pm \mu_B B$. This means that the original transition energy between two terms will split into three transition energies due to the Zeeman effect: one greater than the original energy by $\mu_B B$, one equal to the original energy, while the last one less than the original energy by $\mu_B B$. As a result, the original spectral line that corresponds to such a transition will split into three separate lines, one of them coinciding with the original line. Notice that the new spectral line with a smaller wavelength (larger transition energy) corresponds to $\Delta M_J = 1$, and thus to right-circularly polarized light when viewed from the +z axis. For the same reason, the new spectral line with a larger wavelength should correspond to left-circularly polarized light, while that with the same wavelength as the original line should correspond to linearly polarized light polarized along the z axis.

2.2.3 The anomalous Zeeman effect

The anomalous Zeeman effect refers to when a spectral line splits into more than three separate lines under the external magnetic field.[9] This can occur when the total spin quantum number S for the initial and final states are not zero. In this case, the Landé g factor for a term, as in Equation 5, does not equal to 1 in general. Suppose an atom transitions from State 1 to State 2. Then the extra transition energy contributed by the anomalous Zeeman effect, as shown in Equation 6, can be written as

$$\Delta E_z = f(g_1, g_2) \mu_B B \tag{8}$$

where $f(g_1, g_2) = g_2 M_{J_2} - g_1 M_{J_1}$. In this case, although by the selection rules ΔM_J can only takes 0 and ± 1, $f(g_1, g_2)$ does not need to equal ΔM_J as in the normal Zeeman effect. Therefore, there will in general be more than three different Zeeman energies under the anomalous Zeeman effect, and hence more than three spectral lines will appear in general.

2.3 The cadmium red line

In this experiment, we will observe the cadmium red line (643.85nm) and its splitting under an external magnetic field. A neutral cadmium atom has two valence electrons with $5s^2$ being the their ground configuration. The cadmium red line corresponds to a transition for the valence electrons from 5s5d ($^1D_2$) to 5s5p ($^1P_1$)[10]. Since the total spin quantum number S equals zero for this transition (2S+1=1), an external magnetic field should lead to the normal Zeeman effect. Therefore, under a relatively weak external magnetic field, a spectral line for this transition should split into three separate lines, with the new central line coinciding with the original line. The diagram for this scenario is shown in Figure 1

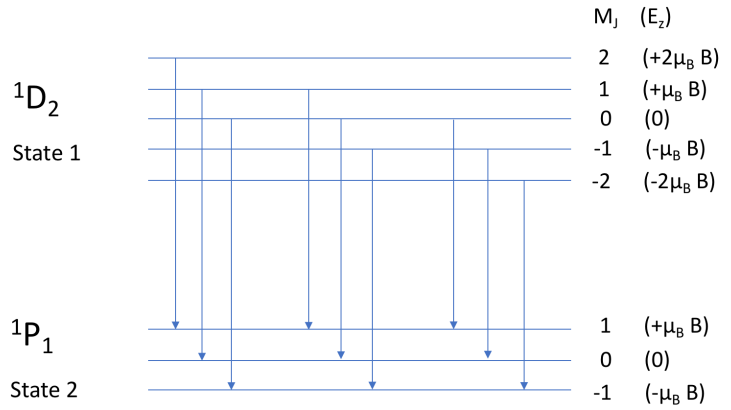

Figure 1: A diagram for the cadmium red line transitions under a weak external magnetic field.

2.4 The mercury green line

In this experiment, we will also observe the mercury green line (546.08nm) and its splitting under an external magnetic field. A neutral mercury atom has two valence electrons with $6s^2$ being their ground configuration. The mercury green line corresponds to a transition for the valence electrons from 6s7s ($^3S_1$) to 6s6p ($^3P_2$).[11] The Landé g factors for the initial (State 1) and the final (State 2) states are 2 and $\frac{3}{2}$, respectively, according to Equation 5. This reflects the anomalous Zeeman effect. Figure 2 shows this transition scenario, and Table 1 lists the Zeeman energies for all the possible transitions. As shown in Figure 2 and Table 1, there are nine different transitions associated with the mercury green line, all with different transition energies. Therefore, the original mercury green line should split into nine separate spectral lines.

2.5 Lummer-Gehrcke plate

In this experiment, we will use a Lummer-Gehrcke plate (also called a Lummer-Gehrcke interferometer) to observe the spectral lines of cadmium and mercury. As shown in Figure 3, a Lummer-Gehrcke plate (I will call it **LG plate**) is a fused-quartz glass plate with extremely flat and parallel surfaces. As shown in the figure, light would pass into the plate through a prism, and will reflect back and forth in the plate at an angle slightly less than the **critical angle**, if larger than which there would be a **total internal reflection** and no light could transmit out of the LG plate. Therefore, every time a light ray inside the LG plate hits the surface of the plate, part of it will transmit out the LG plate at a transmission angle near 90°. Define α to be the transmission angle and θ to be the angle of emergence such that $\theta = 90° - \alpha$. As shown in

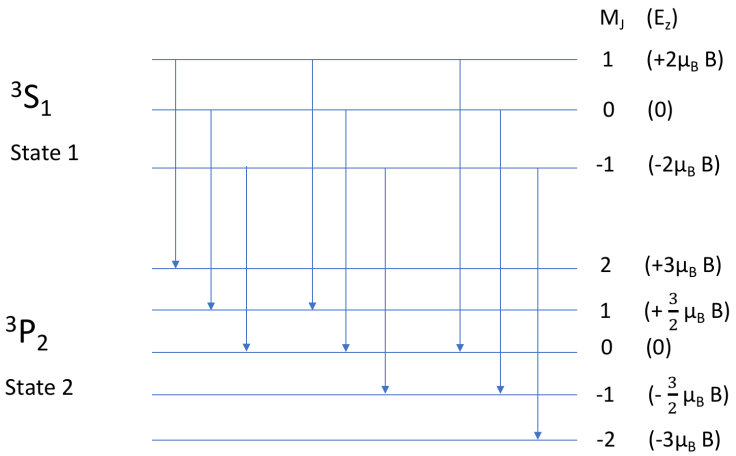

Figure 2: A diagram for the mercury green line transitions under a weak external magnetic field.

Final	Initial	M_2-M_1 (ΔM)	Transition energy shift (μ_B)
M_2	M_1		
0	1	-1	2
-1	0		3/2
-2	-1		1
1	1	0	1/2
0	0		0
-1	-1		-1/2
2	1	1	-1
1	0		-3/2
0	-1		-2

Table 1: A table of all the possible transitions for the mercury green line under a weak external magnetic field.

Figure 3, for a continuous beam of light passing into the LG plate, after many rounds of reflections inside the plate, the transmitted light rays will emerge out of the LG plate in a parallel manner with a very small angle of emergence θ. As shown in Figure 3, suppose there is another incident beam passing into the LG plate with a different angle of incidence on the prism. Then if this beam of light gets transmitted out of the LG plate, it will have a different angle of emergence than the first one. Therefore, light beams entering the LG plate with different incidence angles would correspond to groups of parallelly transmitted light beams with different angles of emergence (if they did get transmitted).

If we place a convex lens at the other end of the LG plate, as shown in Figure 3, then these groups of parallel beams will be converged by the lens at points of different heights. However, for each group of parallelly transmitted light, the transmitted light beams might have different phases with respect to each other. Therefore, when they are finally converged by the lens, these beams might not interfere with each other constructively so as to form a clear image. In fact, it is only for certain discrete incident angles that the corresponding groups of transmitted beams will emerge out of the LG plate in phase and finally interfere with each other constructively to form a clear image. Therefore, for incident beams of monochromatic light with a continuous range of incident angles, an observer, at the other end of the lens, can observe a fringe pattern. Also, as shown in Figure 3, the incident light beams are transmitted out of the LG plate through both the top and the bottom surfaces of the plate so that the observer will indeed observe a vertically

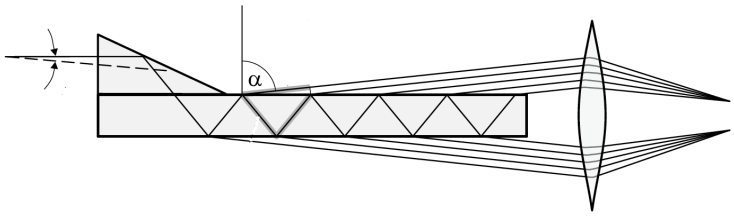

Figure 3: A schematic diagram for the Lummer-Gehrcke plate

symmetric fringe pattern with a blank region between the top and bottom groups of fringes.[12]

Now, let's consider, besides the original beams of monochromatic light incident into the LG plate as just discussed, there is another group of monochromatic incident beams that also enters the LG plate with a continuous range of incident angles. However, the new group of beams have a slightly different wavelength than that of the first group. Therefore, the fringe pattern of the second group of incident beams will be slightly shifted from that of the first group. So, for each fringe due to the first group of light, there will be a new fringe appearing very close to it. Suppose the separation between two original fringes is a. For one of the two original fringes, suppose the distance between itself and its closest neighboring new fringe is s. Then the following relationship can be derived from optics and geometrical arguments:

$$|\Delta\lambda| = \frac{s}{a} \times \frac{\lambda_0^2}{2d} \times \frac{1}{\sqrt{n^2 - 1}} \tag{9}$$

where $\Delta\lambda$ is the difference of wavelength between the two groups of incident beams, λ_0 is the wavelength of the first group of incident beams, d is the vertical thickness of the LG plate, and n is the index of refraction of the LG plate with respect to the wavelength λ_0.[13] Notice that for different wavelengths, the index of refraction of the LG plate can be slightly different.

Lastly, we need to emphasize that Equation 9 gives us a handy method to calculate the difference of wavelengths between different incident beams of light by observing the fringe pattern produced by the LG plate. This is especially useful for observing the change of radiation wavelengths as a result of the Zeeman effect, since the changes of wavelength in Zeeman effect are usually very small compared to the original wavelength.

2.6 The linear polarizer and the quarter-wave plate

In this experiment, we would employ linear polarizers and quarter-wave plates to manipulate the light emitted by cadmium and mercury. A linear polarizer is a filter that will only let a particular polarization direction of the incident light pass through.[14] A quarter-wave plate, in comparison, can convert a linearly polarized light into one that is circularly polarized, and vice versa. A fixed quarter-wave plate will convert left circularly polarized light and right circularly polarized light into linear polarized light of mutually perpendicular directions of polarization.[15]

3 Experiment

3.1 Experimental setup

As shown in Figure 4, the apparatus of this experiment mainly consists of an electromagnet, a cadmium-mercury lamp (Cd-Hg lamp), and an optical system. The electromagnet is composed of two coils of wire with a pole piece on top of each coil. When the power supply of the electromagnet is turned on, a uniform, horizontal magnetic field will be supplied between the two pole pieces. On top of the pole pieces, there is a lamp holder which can fix the removable Cd-Hg lamp between the two pole pieces. The Cd-Hg lamp is connected to another power supply. When this power supply is turned on, the Cd-Hg lamp will radiate light with wavelengths characteristic of cadmium and mercury's spectrum.

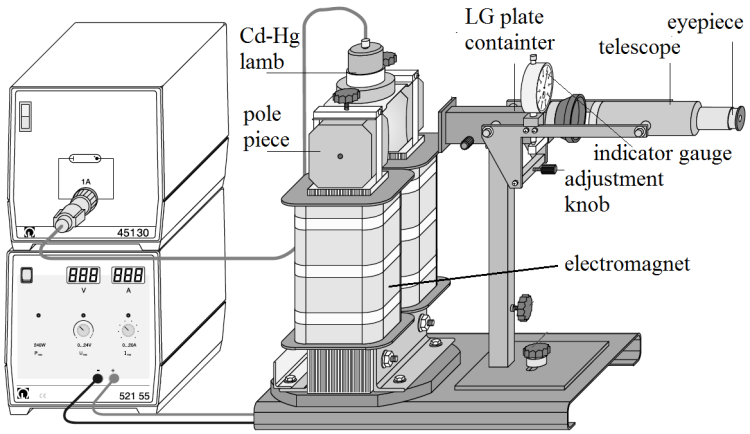

Figure 4: Experimental setup of the Zeeman effect experiment

The optical system is mainly comprised of a Lummer-Gehrcke plate (4mm thick) and a telescope. As shown in Figure 4, the Lummer-Gehrcke plate (LG pate) is placed inside an opaque container such that light emitted from the Cd-Hg lamp can go through a horizontal slit on the one side of the container into the LG plate, and come out through the other side of the container. When light comes out of the container, it will go through a telescope which is focused on infinity. This means that the out-coming parallel light rays can be focused by the telescope before the observer's eye so that a fringe pattern of the light can be observed (see Section 2.5).

Right at the respective ends of the LG plate container and the telescope that are near each other, a quarter-wave plate and a linear polarizer can be mounted. At the other end of the LG plate container, which is close to the Cd-Hg lamp, an optical filter can be mounted. In this experiment, we will only use a red filter and a green filter to isolate wavelengths around the cadmium red line (643.85nm) and the mercury green line (546.1nm) respectively.

Right below the LG plate container, there is an adjustment knob that can adjust the height of the telescope. Beside the LG plate container, there is also an indicator gauge that measures how much the telescope has been moved up or down with the adjustment knob, at a scale of 0.01mm. Moreover, on the eyepiece of the telescope, there is a pair of crosshairs whose crossing point can be used to aim at different fringes on the fringe pattern while the telescope is being adjusted up or down with the adjustment knob. Therefore, the absolute and relative separations between the fringes can be measured with the indicator gauge by aiming the crosshairs at different fringes.

In the experiment, the optical system will be placed such that both the LG plate container and the telescope align with the Cd-Hg lamp horizontally so that light emitted by the lamp can readily go through the LG plate container and the telescope. Moreover, as shown in Figure 5, light from the Cd-Hg lamp will be observed in two directions in this experiment, one parallel to the magnetic field between the pole pieces (**the parallel direction**), and the other transverse to the magnetic field (**the transverse direction**). To facilitate this, the hollow pole pieces have a hole on each side perpendicular to the applied magnetic field so that the optical system can be placed right beside a hole of a pole piece to observe light emitted by the Cd-Hg lamp in the parallel direction (see Figure 5).

Besides the aforementioned major equipment, we will also use a magnetometer to measure the strength of the applied magnetic field between the two pole pieces. Apart from this, there is an ammeter connected between the electromagnet and its power supply so that the current passing through the electromagnet can be monitored. The magnetometer and the ammeter together are used to obtain a calibration of the magnetic field versus the electromagnet current.

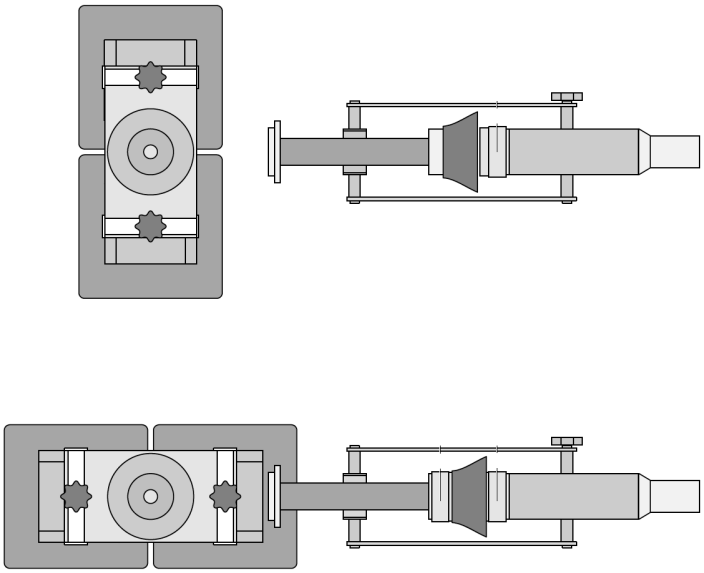

Figure 5: Top view of the relative positioning of the electromagnet and the optical system for observations (top) in the transverse direction (bottom) in the parallel direction.

3.2 Experimental theory

3.2.1 Relationship between the observed fringe separations and the applied magnetic field strength

Suppose that the transition wavelength between two atomic states was originally λ_0, corresponding to a transition frequency of f_0 and an energy difference E_0 between the two states. Then we want to know how much the transition wavelength λ_0 will change as a result of a small change ΔE of the original transition energy E_0. Suppose the new transition frequency is f, then we will have $f = f_0 + \frac{\Delta E}{h}$, where h is the Planck constant. Let the speed of light be c, then we have

$$\begin{aligned}
\Delta\lambda &= \frac{c}{f} - \frac{c}{f_0} \\
&= \frac{c}{f_0 + \frac{\Delta E}{h}} - \frac{c}{f_0} \\
&= \frac{c}{f_0(1 + \frac{\Delta E}{hf_0})} - \frac{c}{f_0} \\
&= \frac{c}{f_0} \times (\frac{1}{1 + \frac{\Delta \mathrm{E}}{E_0}} - 1) \\
&\approx \frac{c}{f_0} \times (1 - \frac{\Delta \mathrm{E}}{E_0} - 1) \\
&= \lambda_0 \times (-\frac{\Delta E}{E_0}) \\
&= \frac{-\lambda_0 \, \Delta \mathrm{E}}{\frac{hc}{\lambda_0}} \\
&= -\frac{\lambda_0^2 \, \Delta \mathrm{E}}{hc}
\end{aligned} \tag{10}$$

Therefore, we have established a relationship between a small change ΔE of the original transition energy E_0 and the corresponding small change $\Delta\lambda$ of the original transition wavelength λ_0. Remember from Section 2.5 that the small change of the original wavelength can be calculated from the fringe pattern created by

the Lummer-Gehrcke plate. From Equation 9, we can see as long as we know the absolute separation a between two adjacent fringes of the original wavelength λ_0 (see Figure 6) and the absolute separation s between one of the two original fringes and its nearest "split-out" fringe due to a change of wavelength $\Delta\lambda$, then we can calculate the absolute change of wavelength $|\Delta\lambda|$ from the ratio $\frac{s}{a}$, since we know the thickness of the LG plate (4mm), the original transition wavelength λ_0, and its associated index of fraction in the LG plate (fused-quartz). In this experiment, however, we will actually locate three adjacent fringes

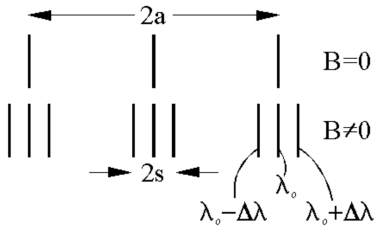

Figure 6: Fringe separations as a result of changes to the transition wavelength λ_0. The wavelength changes illustrated are $\pm\Delta\lambda$.

of the original wavelength (instead of just two) and measure the separation between the two outer fringes $2a$. Similarly, we will locate two "split" fringes (instead of one) around the central fringe of the original triplet and measure the the separation between the two "split" fringes $2s$ (assuming the two "split" fringes correspond to opposite changes to the original transition wavelength). Then the relative separation $\frac{s}{a}$ will just be the ratio $\frac{2s}{2a}$. Notice that we are measuring the fringe separations this way because we want to decrease the percentage error for the fringe separation measurement. Given a certain amount of uncertainty for measuring the position of a single fringe with the indicator gauge, the wider the separation we measure, the less the percentage uncertainty the measured separation will be.

Combining Equation 10 and Equation 9, we can relate the measurable quantity $\frac{s}{a}$ to the absolute energy separation $|\Delta E|$ as:

$$\frac{\lambda_0^2|\,\Delta\mathrm{E}\,|}{hc} = (\frac{s}{a})(\frac{\lambda_0^2}{2d\sqrt{n^2-1}})$$

Rearranging the terms, we obtain

$$\frac{s}{a} = (\frac{2d\sqrt{n^2-1}}{hc})|\Delta E| \tag{11}$$

Now, we want to relate the absolute change of the transition energy $|\Delta E|$ to the applied magnetic field between the pole pieces. Applying Equation 8 in Equation 11, we get

$$\frac{s}{a} = \left(\frac{2d\sqrt{n^2-1}}{hc}|f(g_1,g_2)|\mu_B\right)B \tag{12}$$

Therefore, we have obtained a theoretical relationship between the measurable quantities $\frac{s}{a}$ and B. Notice that the proportionality factor

$$p = \frac{2d\sqrt{n^2-1}}{hc}|f(g_1,g_2)|\mu_B \tag{13}$$

consists of constants and parameters that can be known outside the experiment. Therefore, in order to compare the experimental results from the theory, we can obtain an average proportionality factor p by doing a least squares fitting on the experimental data of $\frac{s}{a}$ vs. B for various strengths of the applied magnetic field, and compare the value of p from least squares fitting to its theoretical value.

3.2.2 Observing the cadmium red line

From now on I will call the fringes without the applied magnetic field the **original fringes**, and those with the magnetic field applied the **new fringes**.

According to Section 2.3, each original red fringe will split into three new fringes with the magnetic field switched on, and $f(g_1,g_2)$ for the "split-out" fringes is ±1. The thickness d of the LG plate is 4mm. For

the cadmium red line wavelength of 643.85nm, the index of refraction n of the LG plate is 1.457.[16] Thus, according to Equation 13, the theoretical value for the p factor is 0.40/T, where the unit T is tesla.

3.2.3 Observing the mercury green line

According to Section 2.4, each original green fringe will split into nine new fringes with the magnetic field switched on. However, in the experiment, it would be hard to observe the fringe splittings clearly since all the nine new fringes would blur together. Notice that, from Table 1, the three central fringes among the nine will correspond to light linearly polarized along the direction of the magnetic field, while the other six lines will correspond to light polarized in the vertical direction. Therefore, in the experiment, we would mount a linear polarizer before the telescope and configure it in a way to filter out the central fringes. Even so, the fringes within the top and the bottom fringe groups would still be hard to distinguish, so in the experiment we would only use the crosshairs to pinpoint the vertically middle points of the top and bottom groups of fringes, and measure the separation between these two points using the indicator gauge. We will treat the middle points of the top and bottom groups as corresponding to the middle fringes of the respective groups. According to Table 1, the middle fringe in the top group will correspond to a change of transition energy $\Delta E = \frac{3}{2}\mu_B B$, while the middle one in the bottom group will correspond to $\Delta E = -\frac{3}{2}\mu_B B$. Therefore, $f(g_1, g_2)$ in this case is $\pm\frac{3}{2}$. Notice that the mercury green line corresponds to an original wavelength λ_0 of 546.08nm, for which the index of refraction n of the LG plate is 1.460. Thus, according to Equation 13, the theoretical value for the p factor in this case is 0.60/T.

3.2.4 Verification of the polarization of light

In this experiment, we will verify the polarization of the emitted light for cadmium.

When we are observing the new fringe patterns in the transverse direction, we expect to observe only linearly polarized light. According to Section 2.2.2, for each original fringe, we expect to observe three new fringes with the central one coinciding with the original fringe. The central new fringe should correspond to light polarized parallel along the magnetic field, while the top and bottom new fringes should correspond to light polarized along the vertical direction. To verify this, we can mount a linear polarizer between the LG plate container and the telescope, and rotate the linear polarizer while observing the new fringes. If we saw the central fringe and the top and bottom fringes appear and disappear alternately, then we could verify that the central fringe is linearly polarized differently from the top and bottom fringes. Notice that we do not know the direction of polarization of the linear polarizer before the experiment.

When we are observing the new fringe patterns in the parallel direction, we expect to see doublets of new fringes that are circularly polarized in different directions (since the z-direction polarized light cannot be seen along the z direction). To verify this, we will mount a quarter-wave plate at the end of the LG plate container and a linear polarizer right before the telescope. If the two lines in a doublet correspond to circularly polarized light but in different directions, then each of them will be linearly polarized transverse to each other. If we fix the quarter-wave plate and rotate the linear polarizer, then we should expect to observe the two lines in the doublet appear and disappear in an alternating sequence, and thus verify that the two lines are circularly polarized in opposite ways. Note that if any line of the doublet were linearly polarized, it would be circularly polarized by the quarter-wave plate and thus rotating the linear polarizer would not prevent us from seeing that line.

3.3 Procedure

3.3.1 Calibrating the magnetic field

With the Cd-Hg lamp out of the lamp holder, we used the magnetometer and the ammeter to measure the magnetic field between the two pole pieces and the electromagnet current simultaneously. We conducted such measurements for multiple voltages on the electromagnet over two trials: one with a gradually increasing electromagnet current while other other with a decreasing one. We also measured the current and the magnetic field, in a new trial, at two extra points with 8 volts and 10 volts of the voltage.

3.3.2 Observing the cadmium red line

First, we placed the optical system to observe the fringe pattern in the transverse direction, with only the red filter mounted and the Cd-Hg lamp between the pole pieces. After this, we turned on the ammeter and the power supplies for the electromagnet and the Cd-Hg lamp, with the power supply for the electromagnet starting at 0 volt. The Cd-Hg lamp was shining. Then we turned off the light of the room and observed the fringe pattern through the telescope, while adjusting the positioning of the optical system (by hand) and the height of the telescope (with the adjustment knob) so that we could see the fringe pattern as clear as possible. After this, we selected three neighboring fringes and measured the distance between the top fringe and the bottom fringe (2a). Then, we increased the voltage on the electromagnet to 6 volts, and we observed new fringes appearing. For each original fringe, there were three new fringes, one coinciding with the original fringe while other other two split away from the original fringe, up and down symmetrically. We chose the central fringe of the aforementioned three neighboring fringes as our reference fringe. Then we recorded the current, and measured the separation between the top and bottom split fringes around this reference fringe (2s). We then increased the voltage by about 1 volt, and recorded the current and the separation $2s$. This process was repeated for voltages of about 8 volts, 9 volts, 10 volts, 11 volts, and 12 volts. We repeated the same process for voltages of 6 volts, 7 volts, and 8 volts again, and for 7 volts one more time.

Right after we finished collecting data in the transverse direction with the magnetic field still applied, we took a time to mount the linear polarizer. Then we observed the fringe pattern while rotating the linear polarizer. We observed that the top and bottom splitting fringes and the central fringes appear and disappear in an alternating sequence. Then we took the linear polarizer off.

Then, we placed the optical system to observe the fringe pattern in the parallel direction. The same procedure for observing the cadmium red line in the transverse direction was carried out, except that we recorded the data at voltages from 5 volts to 12 volts with increments of 1 volt and we did not see any central fringes between any pair of splitting fringes.

Right after we finished collecting data in the parallel direction with the mangetic field still applied, we took a time to mount both the quarter-wave plate and the linear polarizer. Then we observed the fringe pattern while rotating the linear polarizer. We saw that the two splitting fringes appear and disappear in an alternating sequence. Then we took the quarter-wave plate and the linear polarizer off.

3.3.3 Observing the mercury green line

We only observed the fringe pattern for the mercury green line in the transverse direction. The procedure is essentially the same as that for observing the cadmium red line in the same direction, despite a few differences.

(1) As predicted in Section 3.2.3, we did observe very blurred new fringes with the magnetic field applied. Therefore, we mounted the linear polarizer before we started to observe the separation $2s$ in a way that the central groups of fringes would be filtered out. This way we could distinguish the top and bottom splitting groups.

(2) The separation $2s$ was measured with respect to the two vertically middle points of a pair of top and bottom splitting groups (see Section 3.2.3).

(3) We recorded data for voltages from about 6 volts to 12 volts with increments of 1 volt.

4 Data analysis

4.1 Calibration of the magnetic field

According to Section 3.3.1, we obtained the data of the magnetic field strength vs. electromagnet current at multiple voltages in two trials. In the first trial we gradually increased the magnetic field strength, while in the second trial we gradually decreased the magnetic field. The data for both trials are shown in Figure 7. From Figure 7, we can see that the magnetic field strength changes linearly as a function of the current, and the changes are consistent between gradually increasing and decreasing field strengths. Therefore, we will use the data from the first trial to obtain a linear relation between the magnetic field strength (B) and

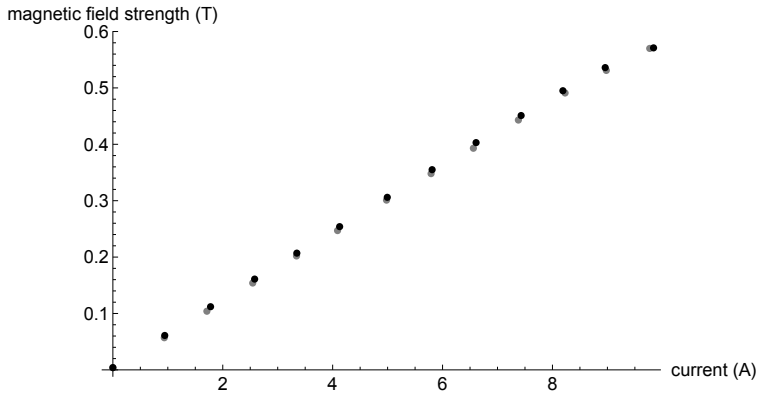

Figure 7: Magnetic field strength vs. electromagnetic current for increasing field strength (gray dots) and decreasing field strength (black dots).

the current (I) with least squares fitting. The least square fitting result is

$$B = (0.05872\text{T/A})I + 0.005267\text{T} \tag{14}$$

where T and A are tesla and ampere. Remember from Section 3.3.1 that, beyond the two main calibration trials, we measured the magnetic field and the current again at 8 volts and 10 volts. The currents at these two voltages are 6.60A and 8.16A, and the corresponding magnetic fields are 0.396T and 0.487T. Using Equation 14 to calculate the magnetic field at 6.60A and 8.16A, we obtain 0.393T and 0.484T. Both calculated values differ from the actual measurements by less than 1 percent. Therefore, for our purpose Equation 14 is accurate enough for calculating the magnetic field given the electromagnet current in repeated resettings of the electromagnet, and we will use this equation to convert the electromagnet current to the magnetic field strength for all subsequent measurements.

4.2 Observation the cadmium red line

4.2.1 Transverse direction

According to Section 3.2.1 and Section 3.3.2, we measured the fringe separation ratio $\frac{s}{a}$ at multiple magnetic field strengths for the cadmium red line in the transverse direction. Remember from Equation 12 and Equation 13 that $\frac{s}{a}$ is proportional to the magnetic field strength B with a proportionality constant p.

$$\frac{s}{a} = pB \tag{15}$$

Therefore, we can determine the constant p by doing a least squares fitting to the data of $\frac{s}{a}$ vs. B, as shown in Figure 8. The least squares fitting result, with $\frac{s}{a} = p_{fit}B$ as the fitting function, gives $p_{fit} = 0.43/\text{T}$. Notice that in this experiment, the magnetic field strengths are calculated from the recorded electromagnet currents with Equation 14 and are accurate to 3 significant figures. The fringe separation ratios $\frac{s}{a}$ are accurate to 2 significant figures in general.

Remember from Section 3.3.2 that right after we finished collecting data for this transverse observation, we watched the fringe patterns when rotating the mounted linear polarizer. Among each group of three new fringes, the central fringe and the two splitting fringes appeared and disappeared in an alternating manner. Then from our arguments in Section 3.2.4, this alternating pattern supports the theory for the normal Zeeman effect that lights emitted transverse to the magnetic field possess polarizations both along and vertical to the magnetic field.

4.2.2 Parallel direction

We also observed the cadmium red line in the parallel direction with a similar procedure as for the transverse direction. The $\frac{s}{a}$ vs. magnetic field strength data along with the least squares fitting line are presented in Figure 9. The corresponding p_{fit} from least squares fitting is $0.40/\text{T}$.

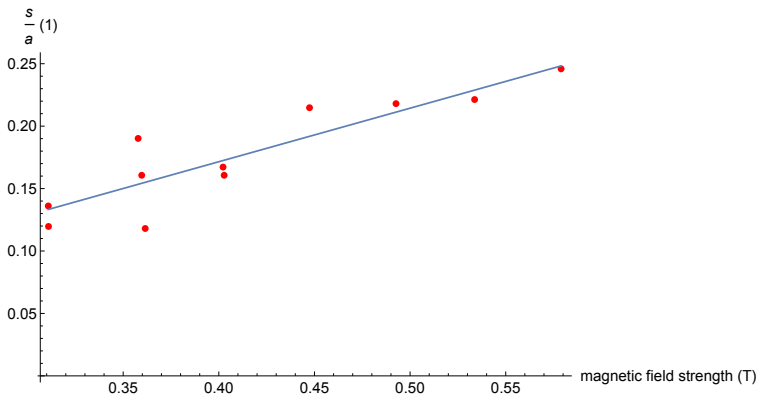

Figure 8: Fringe separation ratio $\frac{s}{a}$ vs. magnetic field strength for observing the cadmium red line in the transverse direction.

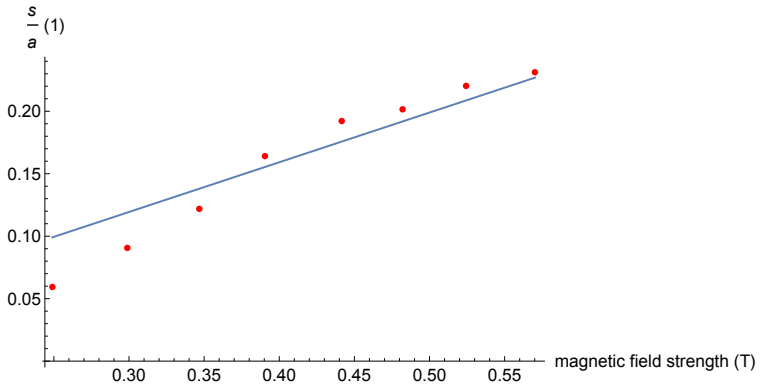

Figure 9: Fringe separation ratio $\frac{s}{a}$ vs. magnetic field strength for observing the cadmium red line in the parallel direction.

Remember from Section 3.3.2 that right after we finished collecting data for this parallel observation, we mounted both the quarter-wave plate and the linear polarizer, and watched the fringe patterns while rotating the linear polarizer. For each pair of splitting fringes, we saw the two splitting fringes appear and disappear in an alternating sequence. This is consistent to our prediction in Section 3.2.4 and proves that the two splitting fringes correspond to lights circularly polarized in opposite directions.

4.3 Observation of the mercury green line

As described in Section 3.3.3, we measured the fringe separation ratio $\frac{s}{a}$ at multiple magnetic field strengths B for the mercury green line in the transverse direction. The $\frac{s}{a}$ vs. magnetic field strength data along with the least squares fitting line are presented in Figure 10. The corresponding p_{fit} from least squares fitting is 0.56/T.

5 Conclusion

In this experiment, we tried to verify the theory of the Zeeman effect with the cadmium red line and the mercury green line. To compare our experimental results with the theory, we defined a proportionality factor p (see Equation 13) that can be calculated with either theoretical derivations or experimental measurements. Besides this, we also tried to verify the theoretical predictions of the light polarization directions involved in the normal Zeeman effect. We will now compare the theoretical and experimental values of p for the cadmium red line and the mercury green line separately.

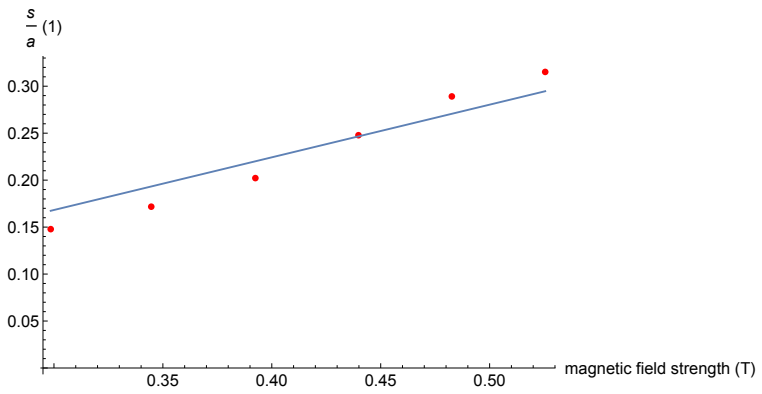

Figure 10: Fringe separation ratio $\frac{s}{a}$ vs. magnetic field strength for observing the mercury green line in the transverse direction.

5.1 The cadmium red line

For the cadmium red line, as described in Section 3.3.2, we observed the fringe pattern with only wavelengths around the cadmium red line filtered through. Besides recording the original triplet fringe separation $2a$, we recorded the new fringe separations $2s$ and the electromagnet currents at various magnetic field strengths. From our analysis of these experimental data in Section 4.2, we obtained $p_{fit} = 0.43/\text{T}$ for the observation in the transverse direction, and $p_{fit} = 0.40/\text{T}$ for the observation in the parallel direction. The p factor from our theoretical prediction for the cadmium red line is 0.40/T. Therefore, the experimental p factor for the transverse observation is greater than its theoretical counterpart by 7.5 percent, while that for the parallel observation agrees with the theoretical value exactly.

According to Equation 15, the experimental errors for the p factor should only come from measurements of the fringe separations $2s$ and $2a$, and the magnetic field strength B. For measurements in both the transverse and parallel directions, the quantity $2s$ is on a scale of 0.1mm, and the quantity $2a$ is on a scale of 0.6mm. Each reading of the indicator gauge (by eye) should have an inherent uncertainty of $\pm$0.001mm, and obtaining one fringe separation required reading the indicator gauge twice (top fringe and bottom fringe). Therefore, each measured fringe separation should have an uncertainty of $\pm$0.002mm. This corresponds to a percentage uncertainty for the separation $2s$ of about $\frac{0.002mm}{0.1mm} = 0.02$, i.e. 2 percent, and a percentage uncertainty for the separation $2a$ of about $\frac{0.002mm}{0.6mm}$=0.003, i.e. 0.3 percent. Therefore, each reading of a fringe separation ratio $\frac{s}{a}$ should have an uncertainty of about 2 percent. Recall from Section 4.1 that each measurement of the magnetic field strength with the aid of Equation 14 should have an error of less than 1 percent. Since $p = \frac{s/a}{B}$ from Equation 15, then each data point in Figure 8 and Figure 9 should correspond to an uncertainty of 3 percent from the inherent inaccuracy of reading the indicator gauge. However, we need to emphasize that in the experiment it was hard to pinpoint each fringe line in an exact manner. The splitting fringe lines we selected in the experiment have a width, on a typical scale, about one third of the separation $2s$, and the crossing point of the cross hair was sometimes hard to pinpoint. Therefore, each measurement of the separation $2s$ could be off by about $\frac{1}{4} \times \frac{1}{3} \times 2 = \frac{1}{6}$ of the true value (each reading of a fringe line position could be off by a quarter of the line width, each line width is about one third of $2s$, and we have two readings for a separation $2s$). This would contribute an uncertainty of about 17 percent to the separation ratio $\frac{s}{a}$ and hence the experimental p factor. Since the separation $2a$ is about sixth times larger than the separations $2s$, the same source of uncertainty for measuring $2a$ would not be as great. Therefore, the inherent difficulty of pinpointing the splitting fringe lines perfectly would be the major source of error for our experimental result, with an uncertainty contribution of about 17 percent.

Understanding this, we can see that our actual experimental error for the p factor for the transverse direction, which is 7.5 percent, is reasonable under the experimental conditions. For the parallel direction, it is fortuitous that the experimental p factor matches the theoretical prediction perfectly. As we can see in Figure 9, the data points do not lie perfectly along the least squares fitting line, but the errors from the individual data points cancel out to give an accurate overall result.

5.2 The mercury green line

For the mercury green line, we only observed the fringe pattern in the transverse direction. The observation procedure is very similar to that of observing the cadmium red line in the transverse direction, despite a few differences described in Section 3.3.3. According to Section 4.3, the experimental p factor was determined to be 0.56/T, while the theoretically predicted p factor is 0.60/T. Therefore, the experimental value is less than its theoretical counterpart by about 7 percent. For mercury's fringe pattern, the separation $2s$ is typically about twice the width of the top or bottom group of splitting lines. Since we were trying to pinpoint the vertically middle point of each of the two splitting groups, from the same argument employed for analyzing the results for cadmium, the uncertainty from the inherent difficulty to pinpoint the middle point of a splitting group is about $2 \times \frac{1}{4} \times \frac{1}{2} = 0.25 = 25$ percent. As in our measurements for the cadmium red line, this uncertainty shall be the major source of error. Therefore, the actual experimental error of 7 percent should be reasonable.

5.3 Overall

As discussed above, the dominant source of the experimental errors is the inherent difficulty to pinpoint the crosshairs exactly at the desired positions of the fringe lines. To ameliorate this situation, it might be desirable to focus the measurements on relatively larger magnetic field strengths so that the fringe separations would be larger. When the fringe separations become larger, the effect of the inaccuracies in measuring the positions of the boundary fringe lines would be smaller, and from our previous reasoning the uncertainty contribution of this dominant source of error to the experimental p factor would also be smaller.

Besides comparing the experimental and the theoretical p factors, we also verified the polarization directions of the light in the transverse and the parallel directions. As discussed in Section 4.2 and Section 2.4, we verified the theoretical prediction, using the cadmium fringe patterns, that lights emitted parallel to the magnetic field should have opposite circular polarizations while those emitted transverse to the magnetic field should have linear polarizations along different directions.

References

[1] B. H. Bunch and A. Hellemans, *The history of science and technology: a browser's guide to the great discoveries, inventions, and the people who made them, from the dawn of time to today* (Houghton Mifflin Harcourt, New York, 2004), pp. 451–456.

[2] C. J. Foot, *Atomic physics* (Oxford University Press, New York, 2005), pp. 13–16.

[3] I. Falconer, The British journal for the history of science **20**, 241–276 (1987).

[4] B. H. Bunch and A. Hellemans, *The history of science and technology: a browser's guide to the great discoveries, inventions, and the people who made them, from the dawn of time to today* (Houghton Mifflin Harcourt, New York, 2004), p. 498.

[5] *The nobel prize in physics 1902*, `https://www.nobelprize.org/nobel_prizes/physics/laureates/1902/`.

[6] C. J. Foot, *Atomic physics* (Oxford University Press, New York, 2005), pp. 80–84.

[7] C. J. Foot, *Atomic physics* (Oxford University Press, New York, 2005), pp. 90–91.

[8] C. J. Foot, *Atomic physics* (Oxford University Press, New York, 2005), p. 90.

[9] S. T. Thornton and A. Rex, *Modern physics for scientists and engineers* (Cengage Learning, Boston, MA, 2012), p. 253.

[10] *NIST atomic spectra database lines data, Cd I*, `https://physics.nist.gov/cgi-bin/ASD/lines1.pl?spectra=cd+i&limits_type=0&low_w=&upp_w=&unit=1&submit=Retrieve+Data&de=0&format=0&line_out=0&en_unit=0&output=0&bibrefs=1&page_size=15&show_obs_wl=1&show_calc_wl=1&unc_out=1&order_out=0&max_low_enrg=&show_av=2&max_upp_enrg=&tsb_value=0&min_str=&A_out=0&intens_out=on&max_str=&allowed_out=1&forbid_out=1&min_accur=&min_intens=&conf_out=on&term_out=on&enrg_out=on&J_out=on`, (accessed: 02.26.2018).

[11] *NIST atomic spectra database lines data, Hg I*, https://physics.nist.gov/cgi-bin/ASD/lines1.pl?spectra=hg+i&limits_type=0&low_w=&upp_w=&unit=1&submit=Retrieve+Data&de=0&format=0&line_out=0&en_unit=0&output=0&bibrefs=1&page_size=15&show_obs_wl=1&show_calc_wl=1&unc_out=1&order_out=0&max_low_enrg=&show_av=2&max_upp_enrg=&tsb_value=0&min_str=&A_out=0&intens_out=on&max_str=&allowed_out=1&forbid_out=1&min_accur=&min_intens=&conf_out=on&term_out=on&enrg_out=on&J_out=on, (accessed: 02.26.2018).

[12] M. Born and E. Wolf, *Principles of optics: electromagnetic theory of propagation, interference and diffraction of light*, 7th ed. (Cambridge University Press, Cambridge, UK, 2003), pp. 380–386.

[13] *Zeeman effect*, https://www.physi.uni-heidelberg.de/Einrichtungen/FP/anleitungen/F44.pdf, (accessed: 02.26.2018).

[14] E. Hecht, *Optics*, 5th ed. (Harlow, England, 2017), p. 346.

[15] E. Hecht, *Optics*, 5th ed. (Harlow, England, 2017), p. 370.

[16] W. S. Rodney and R. J. Spindler, JOSA **44**, 677–679 (1954).